nature geoscience

LETTERS

PUBLISHED ONLINE: 27 FEBRUARY 2011 | DOI: 10.1038/NGEO1089

Weakness of the San Andreas Fault revealed by samples from the active fault zone

B. M. Carpenter*, C. Marone and D. M. Saffer

Understanding the strength and slip behaviour of tectonic faults is a central problem in earthquake physics and seismic-hazard assessment[1–8]. Many major faults, including the San Andreas Fault, are weak compared with the surrounding rock, but the cause of this weakness is debated[1]. Previous measurements of the frictional strength of San Andreas Fault rocks are too high to explain the observed weakness[1,9–13]. However, these measurements relied on samples taken at a distance from the active fault or from weathered surface samples. Recent drilling into the San Andreas Fault[9] has provided material from the actively slipping fault at seismogenic depths. Here we present systematic measurements of the frictional properties and composition of the San Andreas Fault at 2.7 km depth, including the wall rock and active fault. We find that the fault is weak relative to the surrounding rock and that the fault rock exhibits stable sliding friction behaviour. The fault zone contains the weak mineral smectite and exhibits no frictional healing—bonds in the material do not heal after rupture. Taken together, the low inherent strength and lack of healing of the fault-zone material could explain why the San Andreas Fault slips by aseismic creep and small earthquakes in central California, rather than by large, destructive earthquakes.

The apparent weakness of major tectonic faults, as suggested by heat-flow measurements (see for example refs 10,11) and stress orientations (see for example ref. 12), has been widely debated[1]. One of the fundamental unknowns is the absolute magnitude of shear stress acting on faults. Earthquake stress drops are generally between 1 and 10 MPa; however, the shear stress that is relieved during an earthquake is thought to be a small percentage of the absolute fault strength. If the major faults that bound Earth's tectonic plates are strong, shear stresses at seismogenic depths are likely to be 100 MPa or higher, whereas this number could be a factor of 10 or more lower if these faults are frictionally weak.

A number of studies have concluded that the San Andreas Fault (SAF) is mechanically weak[10–12]. Several mechanisms have been proposed, including the presence of weak minerals such as talc[2] or various clays[3], the formation of fabric within the fault zone[4,5] or pore pressure far in excess of hydrostatic[6–8]. Each of these mechanisms is supported by different aspects of a currently incomplete understanding of fault properties at seismogenic depths. One central problem in resolving the debate about the strength of the SAF is that there are no measurements of frictional strength for carefully located samples from the actively slipping fault at seismogenic depths. Existing data are limited to shear zones in the country rock away from the active fault and/or to samples from weathered surface outcrop exposures (Fig. 1a), and indicate friction coefficients of ~0.30–0.55 (refs 15–17), which are considerably higher than those required to satisfy weak-fault models[10–12].

Phase III of the San Andreas Fault Observatory at Depth (SAFOD) drilling project near Parkfield, California, provided direct access to rocks from the active SAF zone. Here, we describe the first friction measurements on samples obtained during SAFOD Phase III drilling through the actively slipping fault. Sample locations are constrained by borehole logging and by direct correlation of the cuttings with core obtained across the active fault (Hole G, Core Runs 4–6; ref. 13).

The SAFOD borehole (Fig. 1a) penetrated two actively creeping strands of the SAF at approximately 2.7 km vertical depth, returning cuttings and core of the wall rock and fault zone. Geophysical logs indicate a ~200-m-wide damage zone characterized by low seismic velocity and electrical resistivity surrounding two active fault strands (Fig. 1a inset). The lower fault strand, at 3,296.3–3,298.9 m drilling depth, is the wider of the two and accommodates nearly all fault motion (Fig. 1b; ref. 13). Core from this fault contains highly sheared rock with penetrative fabric characterized by clay coatings and striations (Fig. 1c; ref. 13). Wall rock southwest of the fault consists of a sheared sandstone and siltstone sequence; rock northeast of the fault consists of highly sheared siltstone and mudstone.

We conducted measurements on cuttings returned from the lower fault and surrounding wall rock. The relative depths of the cutting samples are known with high precision (to within ~0.5 m); however, absolute locations are less well constrained owing to uncertainties associated with drilling-mud circulation times. We use two approaches to locate the cuttings relative to the active fault zone, and to accurately register the cutting depth (CD) in a reference frame of measured depth, as defined from core and geophysical logging data. First, we conducted X-ray diffraction analyses for all cutting samples (Supplementary Fig. S1 and Table S1). Only the sample from the fault zone (at 3,304.8 m CD) contains di-octahedral smectite (montmorillonite), and it is comprised of ~14 wt% smectite. Existing analysis of the intact core recovered from the fault zone also shows that this smectite is found only in the fault rock[18,19]. Second, because we know the measured depths at which drilling began and ended (3,294.9 m and 3,311.8 m, respectively), we can register the cutting depths to these positions and thus to the reported fault-zone depth as defined by analysis of the drill core and downhole logs. Six of our samples (Supplementary Fig. S1) come from the cored interval, drilling depth 3,294.9–3,311.8 m. Two further samples were obtained beyond the cored interval, at 3,317.1 and 3,320.8 m, to ensure that they were from the wall rock to the northeast of the fault. On the basis of these registered depths (herein termed 'cutting depths', CD), we constrain the depth of origin for our cuttings to 3,294.9–3,320.8 m CD, with a sample from the active SAF zone at 3,304.8 m CD.

Samples were washed on site during the drilling operations in a 106 μm sieve and then air-dried. Before our experiments, we ran

Department of Geosciences and Center for Geomechanics, Geofluids, and Geohazards, The Pennsylvania State University, University Park, Pennsylvania 16802, USA. *e-mail: bmc245@psu.edu.

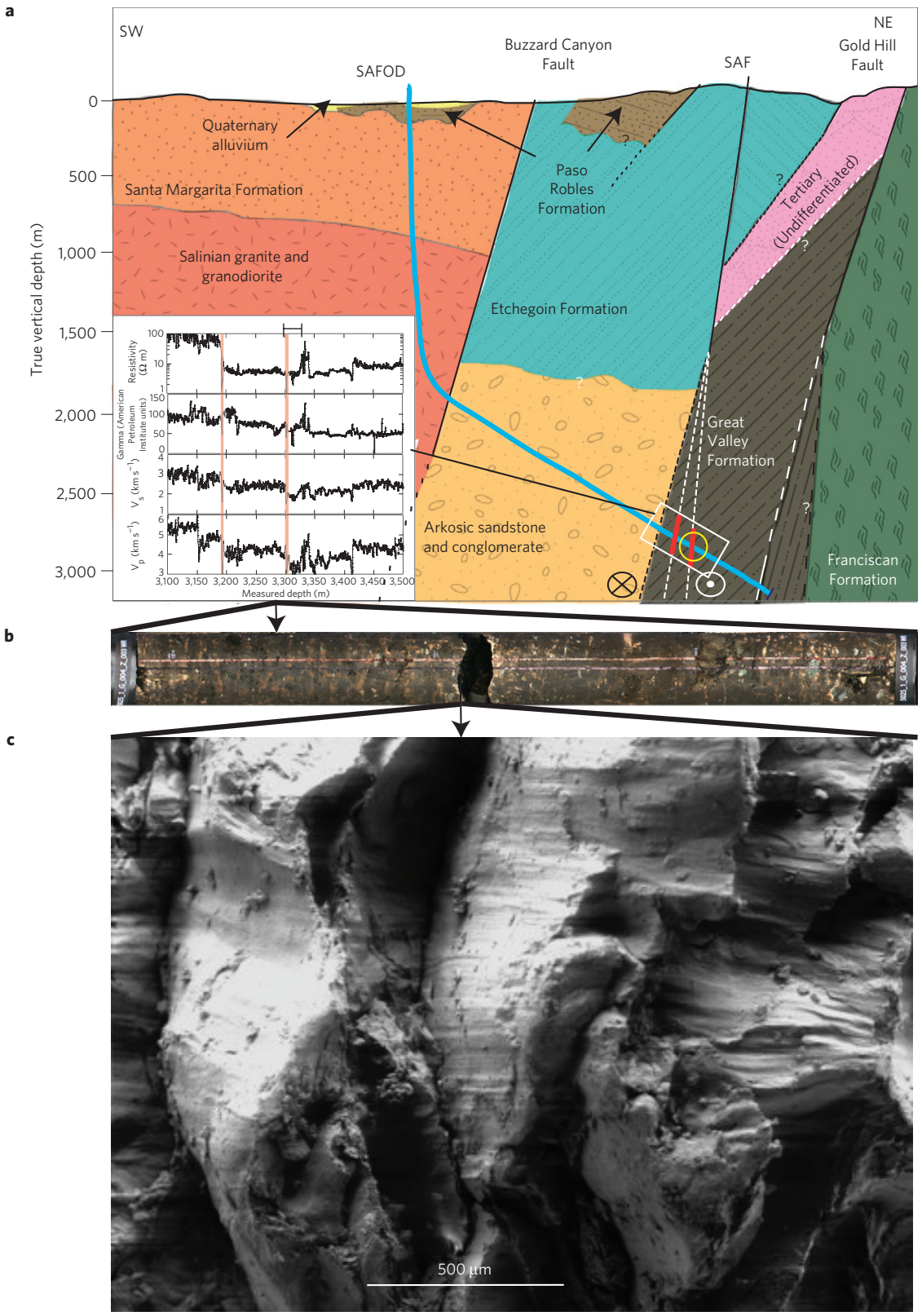

Figure 1 | Geology of the SAF at the SAFOD borehole. a, Geological cross-section[9,14] at the SAFOD borehole (blue line)[9,14], showing cored fault strands (red lines), locations of cuttings used in this study (yellow circle) and the approximate boundary of the geophysical logs (black box). Inset: Geophysical logs from SAFOD Phase II borehole. Red lines indicate active fault strands and the bracket (at the top) indicates the approximate locations of the drill cuttings we studied. **b**, SAFOD Phase III, Hole G, Run 4, Section 3 core from the main creeping strand of the SAF (ref. 13). **c**, Transmission scanning electron microscope image taken from a gap in the core showing anastomosing shear zones in clay-rich foliated gouge[13].

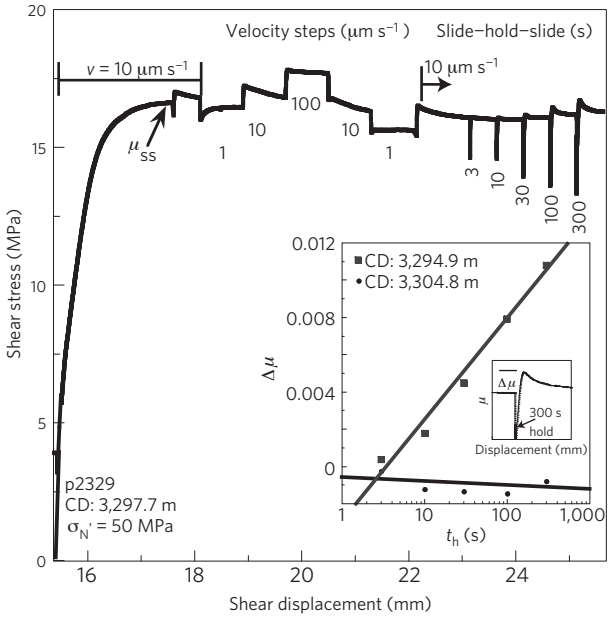

Figure 2 | Experimental data and frictional-healing determination. Raw data for a representative shearing experiment run at an effective normal stress σ_N' of 50 MPa. After a 'run-in' at loading rate $v = 10\,\mu m\,s^{-1}$, velocity steps are used to evaluate the frictional velocity dependence, followed by a slide–hold–slide sequence used to measure the rate at which the peak friction increases with hold time (so-called frictional healing). Larger inset: Frictional healing ($\Delta\mu$) plotted versus hold time (t_h) for two samples. The lines show the best-fit healing rates. Smaller inset: Enlargement of a data segment from the main plot showing the frictional healing parameter $\Delta\mu$.

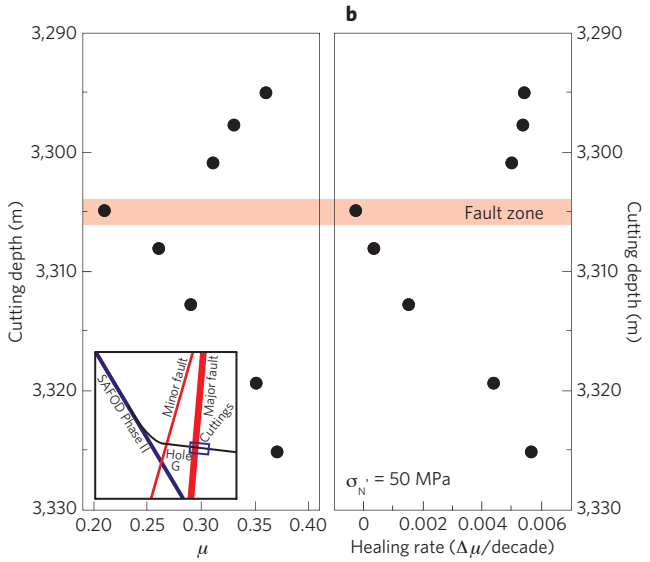

Figure 3 | Frictional strength and healing behaviour. a,**b**, Coefficient of friction (**a**) and healing rate (**b**) as a function of location across the fault zone. The frictional strength and rate of frictional healing are significantly lower in the fault zone compared with the adjacent wall rock. Inset: Schematic diagram of SAFOD boreholes in relation to the active SAF strands and the cuttings studied here.

a magnet through the cuttings to remove metal filings, crushed them, and passed fragments through a 125 μm sieve. We carried out friction experiments in a servo-controlled, true-triaxial pressure vessel (Supplementary Fig. S2; ref. 20) using the double-direct shear geometry in which two layers of material are sheared simultaneously between roughened forcing blocks. We prepared 5-mm-thick layers and sheared them under saturated, drained conditions at constant effective normal stress of 50 MPa, while holding confining pressure and pore pressure constant at 6 MPa and 5 MPa, respectively. Our pore-fluid chemistry matched the natural formation concentrations of Na^+, Ca^{2+}, K^+ and Cl^- measured in the SAFOD borehole[21].

We began each experiment with a run-in of at least 2 mm at a constant displacement rate of $10\,\mu m\,s^{-1}$, to attain steady-state frictional behaviour (Fig. 2). We report values of sliding friction (μ) as the ratio of shear stress to effective normal stress (assuming zero cohesion), taken after this run-in. After reaching a steady state, we conducted velocity step tests and slide–hold–slide tests to quantify (1) the velocity dependence of steady-state friction (Fig. 2) and (2) the frictional healing rate, as measured by the change in frictional yield strength with time (Fig. 2 inset). In velocity step tests, we toggled the load-point velocity between 1 and $100\,\mu m\,s^{-1}$ to measure the friction rate parameter, $(a-b) = \Delta\mu_{ss}/\Delta \ln V$ (ref. 22), where a is the direct effect, b the evolution effect, μ_{ss} the steady-state coefficient of friction and V the loading rate. Positive values of this parameter mean that friction increases with sliding velocity, indicating velocity-strengthening behaviour consistent with stable fault creep. Negative values indicate velocity-weakening frictional behaviour, which is a necessary condition for nucleation of unstable slip and earthquakes. Slide–hold–slide tests are carried out by driving the load point at $10\,\mu m\,s^{-1}$, holding it motionless for a prescribed time t_h (1–300 s) and then driving the load point at $10\,\mu m\,s^{-1}$ again. We report healing rates as $\Delta\mu/\log t_h$, where $\Delta\mu$ is the change in peak friction (Fig. 2 inset). Frictional healing is a key parameter in the seismic cycle and dynamic restrengthening during earthquake rupture. Positive healing rates indicate material strengthening during hold periods, whereas healing rates of zero or below indicate time-dependent weakening.

Our results show that frictional strength varies systematically across the fault zone, and is lowest within the actively creeping fault (Fig. 3a). The friction coefficient is only 0.21 for samples from the fault zone (CD 3,304.8 m) and remains low over a range of effective normal stresses (Supplementary Fig. S3a). Friction for cuttings from the wall rock ranges from 0.30 to 0.37. These values are broadly consistent with those reported for samples from the vicinity of the fault in previous studies[15–17]. The friction rate parameter $(a-b)$ does not vary significantly across the fault, and the fault zone and wall rock both exhibit velocity-strengthening behaviour, consistent with observations of aseismic creep along this portion of the SAF (Supplementary Fig. S3b).

We also observe systematic differences in frictional healing for the fault zone relative to the wall rock (Fig. 3b). Wall-rock samples are characterized by healing rates of up to ~0.006, whereas cuttings from within the fault exhibit essentially zero healing rates (Fig. 3b). We interpret the lack of healing to indicate that grain contact strength does not increase with hold time, which would also contribute to low values of the absolute frictional strength of the fault zone.

The frictional weakness of the fault zone relative to the wall rock correlates with the presence of smectite (Supplementary Fig. S1). In this respect, our results for frictional strength, velocity dependence and healing behaviour are consistent with previous research on synthetic mixtures and natural clay gouges[20,23]; the friction value for the fault zone, $\mu = 0.21$, is similar to values obtained for mixtures of smectite and quartz conducted under similar experimental conditions ($\mu = 0.19$–0.23; ref. 20). Likewise, the velocity dependence of friction ($a-b = 0.0119$–0.0212) we measure for the fault zone cuttings is similar to values reported for synthetic mixtures of smectite and quartz and for pure smectite at similar normal stresses[20,23]. Our results also agree with previous work showing near-zero healing rates in clay-rich fault gouges[24].

Our results carry significant implications for both the weak-fault debate and the slip behaviour of the SAF. We find that material from the actively creeping SAF is weak both in an absolute sense and relative to the adjacent country rock; this is probably due to the presence of smectite localized to the fault zone. The near-zero rate of frictional restrengthening for the active fault zone should further contribute to its both absolute and relative weakness throughout the seismic cycle. Taken together with previous measurements on formations representative of wall rock throughout central California (ref. 25), our results suggest that the SAF is intrinsically weak compared with its wall rock, but the values of friction coefficient we report are not sufficiently low to fully explain the heat-flow and stress-orientation data, which may require a friction value as low as ~0.1. One possibility is that mineral fabric not present in our remoulded samples could result in lower friction[4,5]. For example, existing studies indicate that fault slip occurs within a zone ~2.5 m wide at SAFOD and that most of this is accommodated along localized zones containing higher abundances of smectite, possibly present as authigenic growths that form grain coatings[26] or coat slip planes[19]. However, pure smectite is unlikely to remain stable above ~120–150 °C, and therefore is unlikely as a sole explanation for the apparent low strength of the SAF averaged over seismogenic depths. Alternatively, fault weakness may result from a combination of low intrinsic frictional strength and elevated pore pressure, which would serve to reduce the effective normal stress[27]. Preliminary analysis of core samples from the fault zone suggests both low permeability and a complex pore pressure history including periods of high pore pressure throughout the seismic cycle[19].

Our observations of velocity-strengthening frictional behaviour and near-zero rates of frictional healing also hold important implications for fault-slip behaviour. Most notably, the section of the SAF near the SAFOD site fails primarily by creep, with small (moment magnitude $M_w = \sim 2$) earthquakes and seismic tremor at deeper levels[28]. Our results are consistent with these observations, in that neither the fault material nor the wall rock exhibits the necessary condition for frictional instability (velocity-weakening friction). Combined with the fact that the rate of frictional healing is near zero, this suggests that shear stress around the fault should remain low through the seismic cycle, rather than increasing to a failure threshold before slip.

Our work provides the first direct evidence for intrinsically low frictional strength at seismogenic depths on the SAF. We show that material from the actively creeping fault is broadly consistent with weak-fault models. The coefficient of friction for fault-zone material is 0.21, and increases outside the fault zone to 0.30 or more. Samples from both within and directly adjacent to the fault exhibit velocity-strengthening frictional behaviour. Importantly, the rate of frictional healing within the fault zone is near zero, in contrast to material from outside the fault zone. The low frictional strength and zero healing rates for fault-zone material could explain why only small, repeating earthquakes occur along this patch of the SAF. Moreover, the velocity-strengthening character and zero-healing rates within the fault zone could explain why the SAF mainly fails through aseismic creep in central California.

Received 1 June 2010; accepted 24 January 2011; published online 27 February 2011

References

1. Scholz, C. H. Evidence for a strong San Andreas Fault. *Geology* **28,** 163–166 (2000).
2. Moore, D. E. & Rymer, M. J. Talc-bearing serpentinite and the creeping section of the San Andreas Fault. *Nature* **448,** 795–797 (2007).
3. Schleicher, A. M., van der Pluijm, B. A. & Warr, L. N. Nanocoatings of clay and creep of the San Andreas fault at Parkfield, California. *Geology* **38,** 667–670 (2010).
4. Collettini, C., Niemeijer, A., Viti, C. & Marone, C. Fault zone fabric and fault weakness. *Nature* **462,** 907–910 (2009).
5. Niemeijer, A., Marone, C. & Elsworth, D. Fabric induced weakness of tectonic faults. *Geophys. Res. Lett.* **37,** L03304 (2010).
6. Chester, F. M., Evans, J. P. & Biegel, R. L. Internal structure and weakening mechanisms of the San Andreas Fault. *J. Geophys. Res.* **98,** 771–786 (1993).
7. Faulkner, D. R. & Rutter, J. H. Can the maintenance of overpressured fluids in large strike-slip fault zones explain their apparent weakness? *Geology* **29,** 503–506 (2001).
8. Rice, J. R. in *Fault Mechanics and Transport Properties of Rocks* (eds Evans, B. & Wong, T-F.) 475–503 (Academic, 1992).
9. Zoback, M., Hickman, S. & Ellsworth, W. Scientific drilling into the San Andreas fault zone. *Eos Trans. Am. Geophys. Union* **91,** 197–198 (2010).
10. Brune, J. N., Henyey, T. L. & Roy, R. F. Heat flow, stress, and rate of slip along the San Andreas Fault, California. *J. Geophys. Res.* **74,** 3821–3827 (1969).
11. Lachenbruch, A. H. & Sass, J. H. Heat flow and energetics of the San Andreas Fault Zone. *J. Geophys. Res.* **85,** 6185–6223 (1980).
12. Zoback, M. D. *et al.* New evidence on the state of stress on the San Andreas Fault system. *Science* **238,** 1105–1111 (1987).
13. SAFOD, Photographic Atlas of the SAFOD 3 Cores, (http://earthscope.org/es_doc/data/safod/CorePhotoAtlasv3.pdf), version 3, pp. 51, 58 (2007).
14. Thayer, M. R. & Arrowsmith, J. R. Fault zone structure of Middle Mountain, Central California. *Eos Trans. Am. Geophys. Union* **86,** T21A-0458 (2005).
15. Tembe, S. *et al.* Frictional strength of cuttings and core from SAFOD drillhole phases 1 and 2. *Geophys. Res. Lett.* **33,** L23307 (2006).
16. Morrow, C. A., Solum, J., Tembe, S., Lockner, D. & Wong, T-F. Using drill cutting separates to estimate the strength of narrow shear zones at SAFOD. *Geophys. Res. Lett.* **34,** L11301 (2007).
17. Tembe, S., Lockner, D. & Wong, T-F. Constraints on the stress state of the San Andreas Fault with analysis based on core and cuttings from San Andreas Fault Observatory at Depth (SAFOD) drilling phases 1 and 2. *J. Geophys. Res.* **114,** B11401 (2009).
18. Schleicher, A. M., Tourscher, S. N., van der Pluijm, B. A. & Warr, L. N. Constraints on mineralization, fluid–rock interaction, and mass transfer during faulting at 2–3 km depth from the SAFOD drill hole. *J. Geophys. Res.* **114,** B04202 (2009).
19. Holdsworth, R. E. *et al.* Fault rocks from the SAFOD core samples: Implications for weakening at shallow depths along the San Andreas Fault, California. *J. Struct. Geol.* **33,** 132–144 (2010).
20. Ikari, M. J., Saffer, D. M. & Marone, C. Frictional and hydrologic properties of clay-rich fault gouge. *J. Geophys. Res.* **114,** B05409 (2009).
21. Thordsen, J. J., Evans, W. C., Kharaka, Y. K., Kennedy, B. M. & van Soest, M. Chemical and isotopic composition of water and gases from the SAFOD wells: Implications to the dynamics of the San Andreas Fault at Parkfield, California. *Eos Trans. Am. Geophys. Union* **86,** T23E-08 (2005).
22. Marone, C. Laboratory-derived friction laws and their application to seismic faulting. *Annu. Rev. Earth Planet. Sci.* **26,** 643–696 (1998).
23. Saffer, D. M. & Marone, C. Comparison of smectite and illite frictional properties: Application to the updip limit of the seismogenic zone along subduction megathrusts. *Earth Planet. Sci. Lett.* **215,** 219–235 (2003).
24. Bos, B. & Spiers, C. J. Effect of phyllosilicates on fluid-assisted healing of gouge-bearing faults. *Earth Planet. Sci. Lett.* **184,** 199–210 (2000).
25. Carpenter, B. M., Marone, C. & Saffer, D. M. Frictional behaviour of materials in the 3D SAFOD volume. *Geophys. Res. Lett.* **36,** L05302 (2009).
26. Schleicher, A. M., van der Pluijm, B. A., Solum, J. G. & Warr, L. N. Mineralogical characterization of protolith and fault rocks from the SAFOD Main Hole. *Geophys. Res. Lett.* **33,** L21314 (2006).
27. Fulton, P. M. & Saffer, D. M. Potential role of mantle-derived fluids in weakening the San Andreas Fault. *J. Geophys. Res.* **114,** B07408 (2009).
28. Nadeau, R. M. & Guilhem, A. Nonvolcanic tremor evolution and the San Simeon and Parkfield, California, earthquakes. *Science* **325,** 191–193 (2009).

Acknowledgements

We thank S. Haines for X-ray diffraction work and discussions and D. Moore for providing the transmission scanning electron microscope image of the fault-zone material. We also wish to thank N. de Paola and one anonymous reviewer for their comments, which helped improve this manuscript. Finally, we thank S. Hickman, W. Elsworth and M. Zoback for their efforts to initiate and carry out the SAFOD project. This research was funded by the NSF under grants EAR054570, EAR0746192 and OCE-0648331.

Author contributions

All authors contributed to data analysis and writing. B.M.C. conducted experiments and data analysis.

Additional information

The authors declare no competing financial interests. Supplementary information accompanies this paper on www.nature.com/naturegeoscience. Reprints and permissions information is available online at http://npg.nature.com/reprintsandpermissions. Correspondence and requests for materials should be addressed to B.M.C.